Bioorganic & Medicinal Chemistry 17 (2009) 2830–2841

Contents lists available at ScienceDirect

Bioorganic & Medicinal Chemistry

journal homepage: www.elsevier.com/locate/bmc

Design, synthesis, biological evaluation and molecular modelling studies of novel quinoline derivatives against *Mycobacterium tuberculosis* ☆

Ram Shankar Upadhayaya [a], Jaya Kishore Vandavasi [a], Nageswara Rao Vasireddy [a], Vivek Sharma [a], Shailesh S. Dixit [a], Jyoti Chattopadhyaya [b,*]

[a] *Institute of Molecular Medicine, Pune 411 057, India*
[b] *Department of Bioorganic Chemistry, Biomedical Centre, Uppsala University, Box 581, SE-75123 Uppsala, Sweden*

ARTICLE INFO

Article history:
Received 5 November 2008
Revised 11 February 2009
Accepted 15 February 2009
Available online 21 February 2009

Keywords:
ATP synthase
Diarylquinoline
Protein–ligand docking
Anti-tuberculosis drugs

ABSTRACT

We herein describe the synthesis and antimycobacterial activity of a series of 27 different derivatives of 3-benzyl-6-bromo-2-methoxy-quinolines and amides of 2-[(6-bromo-2-methoxy-quinolin-3-yl)-phenyl-methyl]-malonic acid monomethyl ester. The antimycobacterial activity of these compounds was evaluated in vitro against *Mycobacterium tuberculosis* H37Rv for nine consecutive days upon a fixed concentration (6.25 μg/mL) at day one in Bactec assay and compared to untreated TB cell culture as well as one with isoniazide treated counterpart, under identical experimental conditions. The compounds **3**, **8**, **17** and **18** have shown 92–100% growth inhibition of mycobacterial activity, with minimum inhibitory concentration (MIC) of 6.25 μg/mL. Based on our molecular modelling and docking studies on well-known diarylquinoline antitubercular drug R207910, the presence of phenyl, naphthyl and halogen moieties seem critical. Comparison of docking studies on different stereoisomers of R207910 as well as compounds from our data set, suggests importance of electrostatic interactions. Further structural analysis of docking studies on our compounds suggests attractive starting point to find new lead compounds with potential improvements.

1. Introduction

Tuberculosis (TB) infection *(Mycobacterium tuberculosis)* has become a serious worldwide problem, infecting in synergy with human immunodeficiency virus (HIV) infection.[1] It is contagious, transmitted through air and can infect different organs of the human body, although more than 75% of infection is caused in lungs. It is estimated that, about one third of the world's population is infected with this disease.[2] According to the World Health Organization (WHO) approximately 8 million people are believed to have contracted TB annually with almost 2 million deaths.[2] Three developments have made the resurgence in TB especially alarming. The first is its pathogenic synergy with HIV.[3] The overall incidence of TB in HIV-positive patients is 50 times than that of the rate for HIV-negative individuals.[4] The second is the emergence of drug-resistant, multi-drug-resistant TB (MDR-TB)[5] and recently developed extensive drug-resistant tuberculosis (XDR-TB).[6] The third is gradual understanding of the latent phase of this disease. Considering the world-wide TB problems, there is an urgent need to develop relatively inexpensive new drugs to treat this deadly disease, especially the MDR- and XDR-TB strains.

The quinoline class of compounds has shown the promising activity against resistant tuberculosis. Amongst these, diarylquinoline R207910 (called as DARQ from here on), targeted to the proton pump of bacterial ATP synthase has inhibited mycobacterial growth very effectively.[7] Based on sequence analysis of in vitro mutants resistant to DARQ, it has been established that the target of this putative drug molecule is the c subunit in the F_O domain of ATP synthase.[7,8] Also, various mycobacterial species or mutants harbouring different amino acids at locations Ala63 and Ile66 (subunit c) were found to be resistant to DARQ.[8] Based on these analysis the binding site of DARQ has been proposed near Glu61, which is a highly conserved acidic residue site in ATP synthase subunit c family. It has been known for some time now that the corresponding enzyme in *Escherichia coli* has an equivalent aspartic acid at this location, which is involved in proton translocation in the enzyme, along with another crucial residue, arginine (R186 in *M. tuberculosis* and R210 in *E. coli*) from subunit a.[9] Theoretical and structural

Abbreviations: ATP, adenosine triphosphate; MDR, drug-resistant; XDR, extensive drug-resistant; MIC, minimum inhibitory concentration; DMSO, dimethyl sulfoxide; TB, tuberculosis; WHO, World Health Organization; HIV, human immunodeficiency virus; DARQ, diarylquinoline; EDC·HCl, 1-ethyl-3-(3-dimethylaminopropyl) carbodiimide hydrochloride; DBU, 1,8-diazabicyclo-[5.4.0] undec-7-ene; TBAB, *n*-tetrabutylammonium bromide.

☆ NOTE: All amino acid numbering corresponds to *Mycobacterium tuberculosis* ATP synthase subunits a and c, unless otherwise stated.

* Corresponding author. Tel.: +46 18 471 45 77; fax: +46 18 554495.
E-mail address: jyoti@boc.uu.se (J. Chattopadhyaya).

0968-0896/$ - see front matter © 2009 Elsevier Ltd. All rights reserved.
doi:10.1016/j.bmc.2009.02.026

studies on DARQ has led to identification of an intramolecular hydrogen-bond in *RS* stereoisomer, providing it an extra stability over other isomers.[10] Also, docking studies of DARQ (all four stereoisomers) have suggested the important role of hydroxyl (–OH) and *N*,*N* dimethyl ($-N(CH_3)_2$) moiety in binding to the target protein.[11]

Based on this available information, we have performed the structural, chemical and functional analysis of DARQ in order to shed some light on the origin of its antimycobacterial activity by addressing which of the parts of the DARQ molecule is more important as a pharmacophore for the anti-TB activity. Thus, we have divided this molecule into four hemispheres as shown in Figure 1, and have synthesized new series of compounds[12] based on North-East (NE) and South-East (SE) hemispheres of DARQ molecule.

For this purpose, the hydroxy group in the NE part, have been substituted with different amines (compounds **3**–**20**) and different amides of a diacid (compounds **23**–**31**), which can potentially act on binding sites of ATP synthase with different binding ability. The side chain with the *N*,*N*-dimethyl amino terminal of DARQ was removed since, we assumed, both the amines and the amides might act as binding sites to retain the potency of the compounds. The naphthalene moiety of the SE part, which presumably acts as a binding motif with its lipophilic nature, was substituted with different amines (**3**–**20**), and was replaced by the methyl ester group in the amide class of compounds (**23**–**31**). The main reason behind the change of SE oriented naphthalene moiety was to reduce the bulk of the molecule, because once the total volume of the molecule is reduced, the membrane penetration may become more favourable, which may lead to an improved fit into the binding site. We have also performed molecular modelling and docking studies leading to identification of critical binding sites of the target ATP synthase. Interactions between DARQ and its target protein, ATP synthase, is important for its antimycobacterial activity, which in turn would enable us to improve anti-TB activity of our new in-house synthesized molecules.

2. Results

We have so far prepared 27 different 3-benzyl-6-bromo-2-methoxy-quinoline derivatives and amides of 2-[(6-bromo-2-methoxy-quinolin-3-yl)-phenyl-methyl]-malonic acid monomethyl ester as two potential classes of compounds. Specific procedures followed for all reported compounds along with the respective yields are shown in Table 1. The % inhibition profile of each compound against *M. tuberculosis* H37Rv in vitro is described in Table 2.

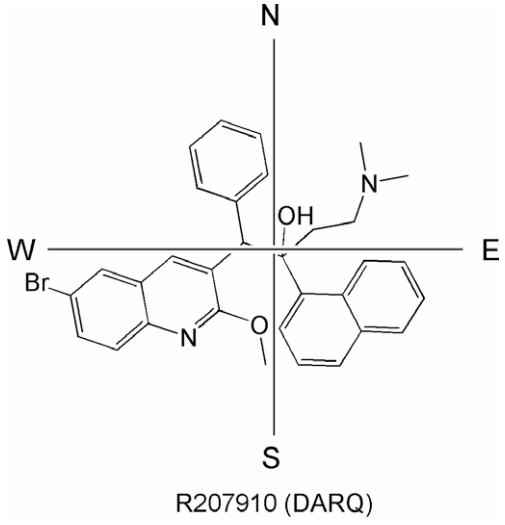

Figure 1. Four different Hemispheres of the molecular structure of highly active R207910 (DARQ)[7] is shown.

2.1. Synthesis

The compounds were prepared using the synthetic sequence illustrated in Scheme 1. 3-Benzyl-6-bromo-2-methoxy-quinoline (**1**), was prepared according to literature procedure.[13] It was brominated at the benzylic centre using *N*-bromosuccinimide and dibenzoyl peroxide to obtain **2** (81%). The series of compounds **3**–**16** were obtained in 10–59% yields by nucleophilic displacement of bromine with a suitable amine (R–H), (Scheme 1) under the influence of activated potassium carbonate in dry *N*,*N*-dimethylformamide (Procedure A). The amines **17** (pyrazole derivative), **18** (6-amino coumarin derivative), **19** and **20** could not however be synthesized using Procedure A, because of poorer acidic nature of amino-proton of these relatively more basic amines. Hence we employed a relatively more severe condition to generate the respective conjugate base of these amines for bromo displacement in compound **2**. Thus, pyrazole derivative **17** was obtained by heating the bromo compound **2** with pyrazole in toluene at reflux in presence of catalytic amount of phase transfer catalyst, *n*-tetrabutylammonium bromide (TBAB) and 20% aqueous sodium hydroxide solution (51%, Procedure B). We however got only a trace amount of compound **18**, by Procedure B. Hence we modified the procedure by adding a organic base 1,8-diazabicyclo-[5.4.0] undec-7-ene (DBU), a catalytic amount of TBAB, 6-amino coumarin hydrochloride and compound **2**, in toluene at reflux to produce compound **18** in moderate yield (42%, Procedure C). Procedures A, B and C failed completely to give compounds **19** and **20**. Ethyl ester of naphthyl acetic acid when however treated with sodium hydride in dry tetrahydrofuran, followed by addition of bromo compound **2**, gave a diastereomeric mixture of **19** and **20** (19%, Procedure D).

Table 1
Procedures[**] used for the synthesis of compounds (**3**–**31**) and yields obtained

Compd #	Procedure	Time (h)	Temperature	Yield (%)
3–16	A	2	80 °C	10–59
17	A	2	80 °C	NR[*]
	B	12	110 °C	51
18	A	2	80 °C	NR[*]
	B	12	110 °C	Traces[#]
	C	12	110 °C	42
19	A	2	80 °C	NR[*]
	D	6	rt	10
20	A	2	80 °C	NR[*]
	D	6	rt	9
23	E	16	rt	27
24	E	16	rt	25
25	E	16	rt	14
	F	16	rt	NR[*]
26	E	16	rt	15
	F	16	rt	NR[*]
27	E	16	rt	14
28	E	16	rt	13
29	F	16	rt	14
30	F	16	rt	30
31	F	16	rt	28

Notes: NR = [*]No reaction. [#]Not isolated.
[**]Procedure A: RH (1 equiv), K_2CO_3 (1.2 equiv), DMF, 80 °C, 2 h; 10–59%; Procedure B: 20% aq NaOH (30 mL), pyrazole (1 equiv), TBAB (10 mol %), dry toluene, reflux, 12 h; 51%; Procedure C: 6-aminocoumarin hydrochloride (1 equiv), DBU (1 equiv), TBAB (18 mol %), toluene, reflux, 12 h; 12%; Procedure D: dry THF, NaH (1.5 equiv), naphthyl acetic acid ethyl ester (1.1 equiv), rt, 6 h, 19%; Procedure E: R in dry THF, NaH (1.2 equiv), 1.5 h, 28 °C, added to **2** (1 equiv) in dry THF, 28 °C, 16 h, 13–27%; Procedure F: RH (1.1 equiv), EDC·HCl (1.2 equiv), HOBt (1.1 equiv), diisopropyl amine (1.2 equiv), THF, rt, 16 h.

Table 2
Description of the compounds synthesized for testing against *M. tuberculosis*, their % inhibition and clog *P*

Compd no.	% Inhibition	clog *P*	Compd no.	% Inhibition	clog *P*
3	94.2	4.69	**17**	99.5	4.96
4	NT	5.50	**18**	92.5	6.19
5	NT	6.00	**19**	0	8.03
6	59	5.06	**20**	0	8.03
7	NT	5.25	**23**	5	4.11
8	100	7.43	**24**	3	4.11
9	53	6.10	**25**	5	4.35
10	69	4.82	**26**	10	4.35
11	14	4.47	**27**	7	4.91
12	18	6.03	**28**	11	4.91
13	16	5.49	**29**	22	4.93
14	17	4.11	**30**	8	6.24
15	08	7.30	**31**	12	6.24
16	14	4.57	Isoniazid	99	−0.8[a]

NT: Not tested.
[a] From PubChem (http://pubchem.ncbi.nlm.nih.gov/). Actual formula and structure of compounds can be seen in Scheme 1.

Synthesis of compounds (**23**–**31**) were also started from the bromo compound **2**. Treatment of **2** with dimethyl malonate in tetrahydrofuran using sodium hydride as a base gave **21** in excellent yield (94%). Selective hydrolysis of one of the methyl esters in **21** was achieved by heating with aqueous potassium hydroxide in methanol[14] at reflux temperature to produce the compound **22** in satisfactory yield (48%). Compound **22** upon treatment with pyrrolidine, 1-ethyl-3-(3-dimethyllaminopropyl) carbodiimide hydrochloride (EDC·HCl), hydroxybenzotriazole (HOB*t*) and diisopropyl amine in tetrahydrofuran (Procedure F) did not furnish compound **25**–**26**. Compounds **23**–**28** were therefore prepared by treating the corresponding amide of malonic acid methyl ester with sodium hydride in dry tetrahydrofuran followed by addition of compound **2** in dry tetrahydrofuran (Procedure E). The compounds **29**, **30** and **31** were synthesized in 14–30% yields by treating a suitable amine (R–H) with **22** using EDC·HCl, HOB*t* and diisopropyl amine in tetrahydrofuran (Procedure F).[15] All the synthesized compounds were fully characterized by ^{1}H NMR, ^{13}C NMR, distortionless enhancement by polarization transfer (DEPT) and mass spectroscopy.

2.2. Microbiology

All compounds **3**–**20**, **23**–**31** and drug references were dissolved in DMSO at a concentration of 6.25 μg/mL and stored at ~4 °C until used.

2.3. Antimycobacterial activity

The compounds **3**–**20** and **23**–**31** were screened against *M. tuberculosis* H37Rv (ATCC 27294) at the single concentration of 6.25 μg/mL by BACTEC 460 radiometric method.[16,17] It has been found that 3-benzyl-6-bromo-2-methoxy-quinoline derivatives (**3**–**20**) have displayed superior anti-TB activity (Table 2) than the amide derivatives of 2-[(6-bromo-2-methoxy-quinolin-3-yl)-phenyl-methyl]-malonic acid monomethyl ester (**23**–**31**). On the basis of the calculated values of growth index (GI) and percentage TB growth inhibition, the four compounds **3**, **8**, **17** and **18** were found to show excellent antimycobacterial activity in the single dose study (administered on day one). We have plotted the graphs for growth index on the day basis for compounds **3**, **8**, **17** and **18** in comparison with first-line tuberculosis treatment regimen, isoniazid[18] (Figs. 2 and 3).

The comparative data of antimycobacterial activity of compounds **3** and **18** with isoniazid clearly shows that compounds **3** and **18** are able to clear the mycobacterial infection within nine days upon single dose administration on the first day. From analysis of graphs plotted for compounds **3** and **18**, it can be seen that the mycobacterial load, upon a single dose administration at day one, never increase from day 1 to day 9, this observation reflects interesting bactericidal nature of our tested compounds.

Based on our data it is clear that antimycobacterial activity of the compounds **3**, **8**, **17** and **18** are comparable to the standard drug isoniazid.[18] Figure 2 reveals that compounds **8** and **17** can reduce the mycobacterial load up to a sterile condition, and no mycobacterial growth has been seen during the 9 days of study with single dose treatment.

Another interesting observation emerged from our study is the fact that the time taken to obtain the zero bacterial load under our experimental condition is different for different compounds. Thus, compounds **8** and **17** can clear the mycobacterial infection within 2 and 7 days, respectively, whereas the frontline drug, isonazid,[18] under identical experimental condition (BACTEC 460 radiometric method)[16,17] can clear the mycobacterial infection within 9 days to attain the same activity profile. We have observed through preliminary BACTEC data that isoniazid has not shown zero growth of *M. tuberculosis*. A possible reason could be that the *M. tuberculosis* develops resistance when exposed to isoniazid for 9 days, which is not the case with compound **8**.

The comparison of percentage (%) growth inhibition (Fig. 3) ability of compounds with respect to standard drug isoniazid, suggests that compounds **3**, **17** and **18** are able to inhibit the *M. tuberculosis* H37Rv 94.2% (±0.2), 99.5% (±0.4) and 92.5% (±2.8), respectively, whereas compound **8** can inhibit the mycobacterial growth 100% (±0). The mycobacterial activity profile of **3**, **8**, **17** and **18** compounds suggests that each compound has a bactericidal effect as there has been no growth in treated control.

Five different concentrations (6.25, 3.25, 1.56, 0.78 and 0.39 μg/mL) were chosen to determine the MIC of compounds **3**, **8**, **17** and **18** against H37Rv strain and was found to be 6.25 μg/mL for each of them (Table 3).

2.4. Molecular modelling and docking

The docking of DARQ (*RS* stereoisomer) in the putative binding site of ATP-synthase subunit a and c suggested that –OH and *N*,*N*-dimethyl moieties may interact with the crucial residues R186 (a subunit) and E61 (c subunit), as shown in Figure 4a. The distance between –O:hydroxyl of DARQ and NH_2 of R186 = 3.6 Å and –N:dimethyl of DARQ and OE2 of E61 deprotonated = 4.3 Å. Only in the case of *RS* stereoisomer these polar parts of DARQ came into the vicinity of the polar areas of protein. The initial docking scores (Intermolecular energies) of all four stereoisomers (*SS*, *SR*, *RR* and *RS*) were comparable, but after forcefield based refinement, interaction energies (van der Waals and electrostatic contributions only) between DARQ and protein was found to be lowest in the case of *RS* stereoisomer (Table S1). Also, as observed in the *RS* stereoisomer docked complex, the non-polar parts of DARQ molecule, that is, naphthyl, phenyl and quinoline aromatic rings were making effective van der Waals interaction with similar parts from the protein (Section 3).

Docking of some of the active and less active compounds from our data set suggested similar interactions to the ones observed for DARQ binding. The highly active compounds **3**, **8**, **17** and **18** docked into the same putative binding site of ATP synthase, are shown in Figure 4 (compounds **3** and **18**). In general all compounds used in docking studies bind effectively in the binding site, but split of docking intermolecular energies suggests that lacking electrostatic contributions could be the reason of their moderate activity (Table S2 and Section 3).

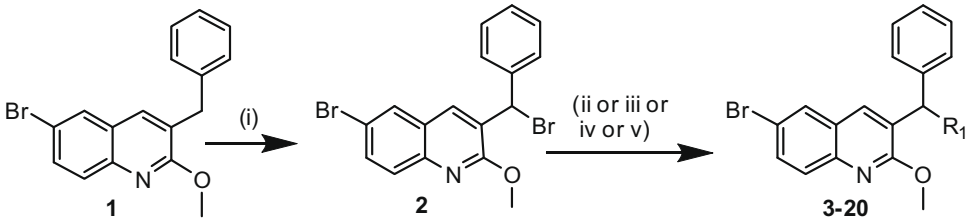

3: R_1 = Imidazolyl (24%); **4**: R_1 = Pyridine 2-ylamine (26%); **5**: R_1 = 6-Methyl-pyridine-2-ylamine (28%); **6**: R_1 = C-(Tetrahydro-furan-2-yl)-methylamine (32%); **7**: R_1 = C-(Thiophen-2-yl)-methylamine (28%); **8**: R_1 = 1-(3-Trifluoromethyl-phenyl)-piperazinyl (49%); **9**: R_1 = Piperidinyl (57%); **10**: R_1 = Morpholinyl (59%); **11**: R_1 = 5-Methyl-tetrazol-1-yl(50%); **12**: R_1 = Pyrrolidine-2-carboxylic acid ethyl ester (11%); **13**: R_1 = Piperidine-4-carboxylic acid ethyl ester (15%); **14**: R_1 = C-Pyridin-4-yl-methylamine (17%); **15**: R_1 = Indolyl (10%); **16**: R_1 = 4-Nitro-imidazolyl (46%); **17**: R_1 = Pyrazolyl (51%); **18**: R_1 = 6-Amino-chromen-2-one (42%); **19**: R_1 = Naphthalen-1-yl-acetic acid ethyl ester (10%); **20**: R_1 = Naphthalen-1-yl-acetic acid ethyl ester (9%)

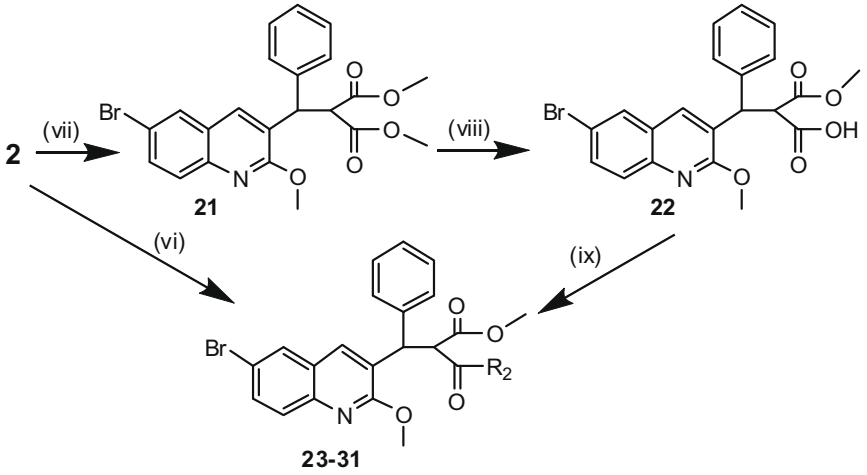

23: R_2 = Morpholinyl (27%); **24**: R_2 = Morpholinyl (25%); **25**: R_2 = Pyrrolidinyl (14%); **26**: R_2 = Pyrrolidinyl (15%); **27**: R_2 = Piperidinyl (14%); **28**: R_2 = Piperidinyl (13%); **29**: R_2 = Pyrazolyl (14%); **30**: R_2 = 1-(3-Trifluoromethyl-phenyl)-piperazinyl (30%); **31**: R_2 = 1-(3-Trifluoromethyl-phenyl)-piperazinyl (28%)

Scheme 1. Reagents and conditions: (i) NBS (1 equiv), dibenzoylperoxide (5 mol %), CCl_4, reflux, 2 h; 81%; (ii) RH (1 equiv), K_2CO_3 (1.2 equiv), DMF, 80 °C, 2 h; 10–59% (Procedure A, for **3**–**16**); (iii) 20% aq NaOH (30 mL), pyrazole (1 equiv), TBAB (10 mol %), dry toluene, reflux, 12 h; 51% (Procedure B, for **17**); (iv) 6-aminocoumarin hydrochloride (1 equiv), DBU (1 equiv), TBAB (18 mol %), toluene, reflux, 12 h; 12% (Procedure C, for **18**); (v) dry THF, NaH (1.5 equiv), naphthyl acetic acid ethyl ester (1.1 equiv), rt, 6 h, 19%; (Procedure D, for **19** and **20**); (vi) R = 3-morpholin-4-yl-3-oxo-propionic acid methyl ester (for **23** and **24**), 3-oxo-3-pyrrolidin -1-yl-propionic acid methyl ester[35] (for **25** and **26**), 3-oxo-3-piperidin-1-yl-propionic acid methyl ester[36] (for **27** and **28**); in dry THF, NaH (1.2 equiv), 1.5 h, 28 °C, added to **2** (1 equiv) in dry THF, 28 °C, 16 h, 13–27% (Procedure E); (vii) NaH (1.2 equiv), dimethyl malonate (1.4 equiv), THF, rt, 4 h; 94%; (viii) aq KOH (1 equiv), MeOH, reflux, 12 h; 48%; (ix) RH (1.1 equiv), EDC·HCl (1.2 equiv), HOBt (1.1 equiv), diisopropyl amine (1.2 equiv), THF, rt, 16 h, (Procedure F, for **29**, **30** and **31**).

2.5. Cytotoxicity

The most active compounds of our data set were also subjected to cytotoxicity assay in two different concentrations at 1 and 10 μg/100 μL. Table 4 lists the percentages of cells viability after 24 and 72 h of addition of compounds. These results are encouraging for further process of our work.

3. Discussion

On the basis of structure functional activity of all these compounds, we assume that the compounds **3** and **17** bearing the imidazole and the pyrazole moiety, respectively, may assist in binding to the active sites favourably. The only difference is the position of the ring nitrogens in these two heterocyclic amines, which evidently do not perturb the lipophilic and lypophobic balance, and thereby showing comparable activity to isoniazid. For compound **18** the main binding site, the secondary amino functionality was buried between the lipophilic portions thereby disturbing the lipophilic–lypophobic balance of the molecule which might have influenced its moderate antimycobacterial activity. When we consider the structure of **8**, it has a tetrahedral space filling with the saturated piperizine ring, where it has nitrogens to act as good binding sites as well as the substituted phenyl ring, which may enhance the potency of the molecule by acting as a binding motif. The phenyl ring also has a reasonable delocalization of charges due to the presence of the polar trifluoromethyl substitution at *meta* position, which provides a better lipophilic–lypophobic balance, and it may favour better binding and penetration ability, thereby influencing the potency of the molecule. All these explained properties makes the molecule **8** potential antimycobacterial agent .

The amides of 2-[(6-bromo-2-methoxy-quinolin-3-yl)-phenyl-methyl]-malonic acid monomethyl ester (**23**–**31**) have not shown

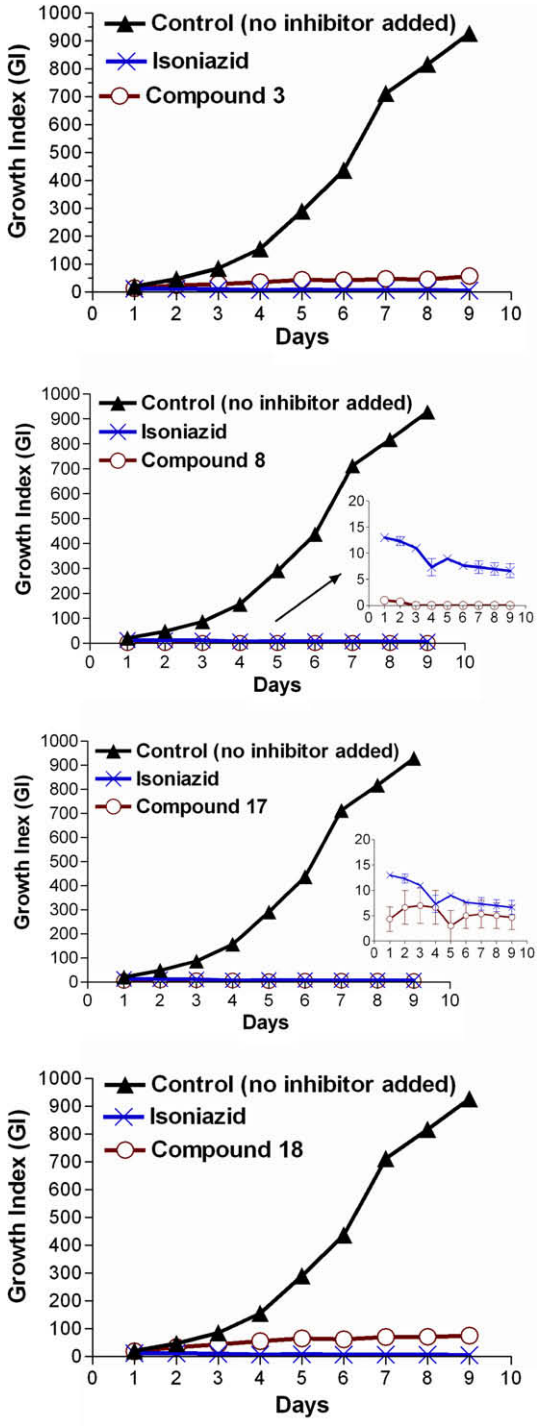

Figure 2. The plot of three independent readings of antimycobacterial growth index (GI), against *M. tuberculosis* H37Rv, are plotted against number of days (day 1 to day 9) for compounds **3**, **8**, **17** and **18** in comparison with isoniazid (internal reference) upon a single dose administration (6.25 μg/mL) at day 1. The standard deviation (SD) of GI in three consecutive readings for **3**, **8**, **17**, **18** and isoniazid have been calculated, please see Table S3 in Supplementary data for details.

significant antimycobacterial activity. The reason may be the unavailability of the binding aptitude of amides.

3.1. Docking studies

Our primary aim in this study was to analyse ligand–protein interactions, based on which we could modify our compounds.

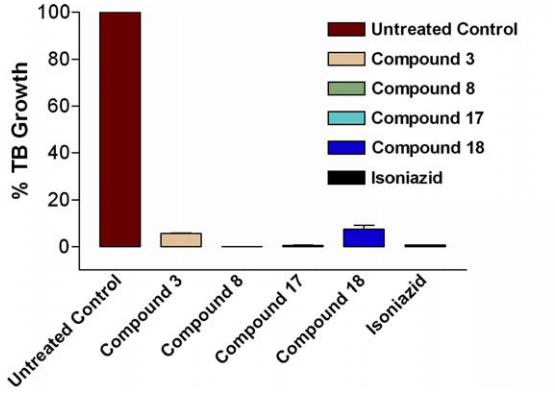

Figure 3. %TB growth inhibition shown for the compounds **3**, **8**, **17** and **18**. Comparison of percentage TB growth inhibition after 7–9 days with control containing no bactericidal agent (left column) and 4 test compounds (**3**, **8**, **17** and **18**) in the middle, while the internal reference compound used in this study is isoniazid. %TB growth inhibition of *M. tuberculosis* H37Rv and the corresponding standard deviation (SD) of three consecutive readings for **3**, **8**, **17**, **18** and isoniazid are, 94.2% (±0.2), 100% (±0), 99.5% (±0.4), 92.5% (±2) and 99.3% (±0.2).

Table 3
MIC of compounds against *M. tuberculosis* H37Rv

Compound	MIC (μg/mL)
3	6.25
8	6.25
17	6.25
18	6.25

All four stereoisomers of the DARQ molecule were modelled and docked into the binding site. The binding site is flanked by transmembrane helices of subunit a and c of the ATP synthase homology model. All 4 stereoisomers docked to the protein with almost similar docking intermolecular energies (Table S2). Clustering (with 2 Å root mean square) was found better for stereoisomers *SR*, *RR*, *SS* than *RS*, but scrutinizing the split of energies showed better van der Waals and electrostatic energy balance in the case of *RS* stereoisomer (Table S2).

Structural analysis suggested that the *RS* stereoisomer was docking into a most acceptable pose. The –OH and $-N(CH_3)_2$ moieties of DARQ were found to be in the vicinity of conserved polar amino acids of subunit a and c (i.e., R186 and E61 of a and c subunit, respectively). The hydrophobic phenyl moiety was placed in the hydrophobic cavity (Leu68 and Phe65 of c subunit) of the protein and making stacking interactions with Phe65 (Fig. 4a). The bulkier, bi-phenyl group was found to make stacking interactions with Tyr64, however, was positioned in slightly polar area. We suggest, the polar substituents at this location on DARQ may increase its efficacy. Further, the quinoline moiety fills the void in the protein and we propose that bromo-group on it would most probably form some halogen bonding interactions and further stabilize the system (unpublished results). These results in contrast to previous docking study[11] suggest the possible role of functional groups of DARQ, other than hydroxyl and *N*,*N*-dimethyl.

The inhibitory effect of DARQ could be that while it sits between the subunit–subunit interface with possible protein–ligand interactions, consequently it does not allow the concomitant rotary movements of the amino acids and the oligomeric C subunit ring.[9] Also we assume that the *N*,*N*-dimethyl moiety could capture a proton and would not allow its transfer to the cytoplasmic side via R186, owing to its comparative pK_a. However, that scenario has not been explicitly modelled in the present study. The possible H-bonding between R186 and –OH moiety of DARQ and interaction

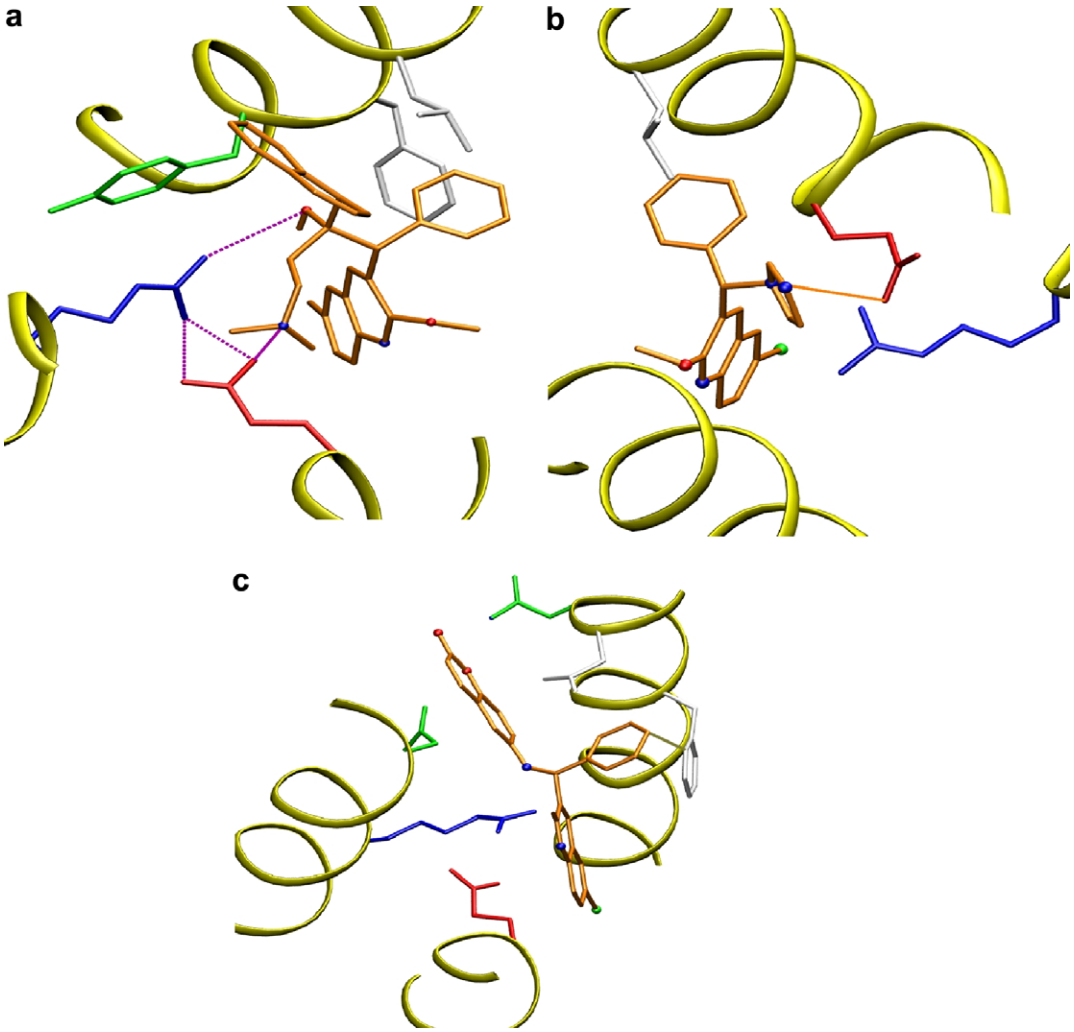

Figure 4. (a) Interactions of DARQ (*RS*) in the binding site of ATP synthase. (b) One active compound **3** from our data set in the binding site of ATP synthase. (c) Another active compound **18** showing similar arrangement as DARQ molecule into the binding site. Arg186 (subunit a) and Glu61 (deprotonated and from subunit c) shown in blue and red, respectively. Non-polar residues in white and polar in green. Ligands (DARQ, **3**, **18**) shown in orange licorice representation. Oxygen, nitrogen and bromine atoms are coloured with red, blue and green schemes. Yellow ribbons representation for the transmembrane helices.

Table 4
Cytotoxic effects of tested compounds on murine macrophage cells after 24 h and 72 h

Compound	10 μg/100 μL		1 μg/100 μL	
	24 h (%)	72 h (%)	24 h (%)	72 h (%)
3	56	67	74	67
8	97	97	87	100
17	75	98	71	100
18	100	100	100	100

of DARQ molecule to all three subunits (two c and one a) could prohibit the regular functioning of the enzyme. In contrast to previous docking study,[11] we suggest that arginine side chain need not flip and still the inhibitory effect of DARQ could be attained.

In comparison, docking simulations on some of our synthesized compounds reveal interesting facts. The docking intermolecular energies and root mean square clustering (2 Å) for both active and less active compounds were found to be not much different from DARQ molecule, however, clearly the electrostatic part of intermolecular energy was prominent only in the DARQ docking simulations and specifically in *RS* stereoisomer (Table S2). This suggests that only space-filling van der Waals interactions may not be critical for antitubercular activity, but they are needed anyway for structural fine-tuning of the ligand in the binding site.

Lowest energy selected conformation of comparatively smaller compound **3** docks in a similar manner (Fig. 4b), however, weaker interactions between imidazole ring and protein and absence of hydroxyl and flexible terminal amine could be the reason of its moderate activity compared to DARQ. The imadazole functional group could act as a potential proton acceptor but to a lesser extent as compared to *N*,*N*-dimethyl, owing to its smaller pK_a value.

Low energy docked pose of compound **8** was structurally similar to DARQ binding, however electrostatic interactions seems to be missing (Table S2). Its piperazine moiety could act as a potential proton acceptor and may have a role in antitubercular activity. The compound **17** is almost similar to **3**, with only heterocyclic ring difference. Another active compound **18**, which is structurally similar to original DARQ molecule sits in a similar arrangement with its aromatic parts in stacking interaction with protein aromatics (Fig. 4c). It has a slightly polar constituent in place of naphthyl moiety of DARQ, which may interact with the Asn190 (subunit a) and Asn67 (subunit c) that could be a factor for its moderate potency, when its secondary amine is buried between two larger substituents. The van der Waals and relatively weaker electrostatic interactions could be prominent for its activity. Similarly other ser-

ies compounds (**3**–**20**), does contain nitrogens, which are protonatable and could make interactions with binding site residues with different strength. The reason for their varying activity could also be associated with their delivery or octanol–water partitioning. The compound **23/24** based on our docking studies fits well into the binding site, but missing electrostatic interactions could be the reason for its in vitro inactivity.

Overall, our preliminary docking studies suggest the phenyl moiety of DARQ could be explored further to larger aromatics, which could make stronger stacking interactions with protein amino acid residues. Also, the halogen could be altered in second round of modifications, which may improve the halogen bonding interactions between the ligand and the protein. Amine and hydroxyl functionality seems to be critical, however, flexible side chains with terminal amines and hydroxyl could be used in our compounds, which could make lesser active compounds potent too.

4. Conclusion

In summary, compounds **3**, **8**, **17** and **18** exhibited moderate to excellent inhibitory activity against *M. tuberculosis*. There is a great similarity in these compounds as all compounds bearing a secondary heterocyclic amine or aryl piperazine except for **18**. The aryl piperizine substituted compound **8** was found to be most active, even better than isoniazid under similar conditions. Although the MIC of these compounds are not as good as the standard drug, isoniazid, the present results have however given us some insight on the importance of the presence of a hydroxy group, the side chain with the *N*,*N*-dimethyl amino terminus and/or the naphthalene moiety, and why they are important for the better antitubercular activity of these molecules. Docking studies speak for the importance of various functional groups of the DARQ molecule, which could help in improving our compounds against TB infection. This we consider as good starting points to improve the design of novel class of anti-tuberculosis molecules.

5. Experimental

5.1. General methods

Purification and drying of reagents and solvents were carried out according to literature procedure.[19] Thin layer chromatographic analyses were performed on E-Merck 60 F 254 precoated aluminium thin layer chromatographic plates. All air-sensitive reactions were carried out under a nitrogen atmosphere. Melting points were determined on a Büchi melting point B-540 instrument and are uncorrected. ^{1}H spectra were recorded on a Bruker Biospin 400 MHz spectrometer and TMS as an internal standard. The values of chemical shifts are expressed in ppm and the coupling constants (*J*) in Hertz (Hz). Mass spectra were recorded in API 2000 LC/MS/MS system spectrometer and the IR spectra were recorded in Perkin Elmer FT-IR spectrometer.

5.1.1. (±)-3-Bromo-3-(bromophenyl methyl)-2-methoxy-quinoline (2)

A mixture of 3-benzyl-6-bromo-2-methoxy-quinoline[13] (**1**, 5.0 g, 15.24 mmol), *N*-bromosuccinimide (2.7 g, 15.24 mmol) and dibenzoyl peroxide (0.18 g, 0.76 mmol) in carbon tetrachloride was heated to reflux for 2 h. The reaction mixture was cooled to room temperature, the solid separated was filtered, the filtrate was concentrated under vacuum, the crude product was triturated with hexane and dried to give the compound **2** (5.0 g, 81%) as an off-white solid, mp 85–86 °C. ^{1}H NMR (400 MHz, $CDCl_3$): δ 4.06 (s, 3H), 6.56 (s, 1H), 7.26–7.38 (m, 3H), 7.44–7.48 (m, 2H), 7.64–7.69 (m, 2H), 7.87 (d, J = 4.0 Hz, 1H), 8.09 (s, 1H). $[M+H]^+$ = *m/e* 406, 408, 410. ^{13}C NMR (100.6 MHz, $CDCl_3$): 48.6, 54.0, 117.5, 126.2, 126.5, 128.29, 128.37, 128.47, 128.6, 129.7, 133.0, 137.5, 139.6, 144.6, 158.6.

5.1.2. Representative Procedure A, for 3–16: Preparation of (±)-6-bromo-3-(imidazol-1-yl-phenyl-methyl)-2-methoxy-quinoline (3)

A mixture of compound **2** (0.300 g, 0.74 mmol), imidazole (0.05 g, 0.74 mmol) and potassium carbonate (0.20 g, 1.47 mmol) in *N*,*N*-dimethylformamide (2 mL) were heated at 80 °C for 2 h. The reaction mixture was poured into ice-water mixture and extracted with ethyl acetate. The organic layer was washed with water, brine and dried over anhydrous sodium sulfate. Organic layer was concentrated under vacuum to get crude product. The crude product was purified by column chromatography on silica gel (100–200 mesh), eluent: hexane–ethyl acetate (7:3, v/v) to afford **3** (0.07 g, 24%) as off-white solid, mp 161–162 °C. ^{1}H NMR (400 MHz, $CDCl_3$): δ 3.97 (s, 3H), 6.82–6.88 (m, 2H), 7.08–7.11 (m, 3H), 7.29 (s, 1H), 7.34–7.38 (m, 3H), 7.41 (s, 1H), 7.67–7.73 (m, 2H), 7.76 (d, J = 1.6 Hz, 1H). ^{13}C NMR (100.6 MHz, $CDCl_3$): δ 54.0, 59.3, 117.7, 119.2, 125.2, 125.9, 127.8, 128.62, 128.63, 128.9, 129.4, 129.7, 133.3, 135.9, 137.3, 137.4, 144.9. $[M+H]^+$ = *m/e* 394, 396.

5.1.3. *N*-((6-Bromo-2-methoxyquinolin-3-yl)(phenyl)methyl) pyridin-2-amine (4)

Procedure A, yield 26%. Oily liquid. ^{1}H NMR (400 MHz, $CDCl_3$): δ 3.99 (s, 3H), 5.22 (d, J = 6.0 Hz, 1H, D_2O exchangeable), 6.14 (d, J = 6.0 Hz, 1H), 6.30 (d, J = 8.0 Hz, 1H), 6.58–6.64 (m, 1H), 7.25–7.40 (m, 6H), 7.62–7.69 (m, 2H), 7.83 (dd, J = 6.8, 2.0 Hz, 1H), 7.99 (s, 1H), 8.06 (d, J = 4.0 Hz, 1H). ^{13}C NMR (100.6 MHz, $CDCl_3$): δ 53.7, 55.7, 107.0, 113.7, 117.3, 126.5, 127.2, 127.4, 127.6, 128.5, 128.6, 129.6, 132.4, 134.5, 137.6, 140.8, 144.5, 148.3, 157.5, 160.4. $[M+H]^+$ = *m/e* 420, 422.

5.1.4. [(6-Bromo-2-methoxy-quinolin-3-yl)-phenyl-methyl]-(6-methyl-pyridin-2-yl)-amine (5)

Procedure A, yield 28%. Oily liquid. ^{1}H NMR (400 MHz, $CDCl_3$): δ 2.60 (s, 3H), 4.08 (s, 3H), 6.04 (d, J = 7 Hz, 1H), 6.50–6.58 (m, 2H), 7.27–7.38 (m, 3H), 7.43–7.50 (m, 2H), 7.58–7.70 (m, 3H), 7.89 (d, J = 1.0 Hz, 1H), 8.08 (s, 1H), 9.40 (br s, 1H, D_2O exchangeable), 15.7 (br s, 1H, D_2O exchangeable). ^{13}C NMR (100.6 MHz, $CDCl_3$): δ 24.2, 53.6, 55.9, 103.0, 113.2, 117.3, 126.8, 127.4, 128.4, 128.6, 129.6, 132.38, 132.42, 134.1, 134.4, 140.7, 141.9, 144.4, 144.5, 157.1, 157.2, 159.8, 160.3. $[M+H]^+$ = *m/e* 434, 436.

5.1.5. [(6-Bromo-2-methoxy-quinolin-3-yl)-phenyl-methyl]-(tetrahydro-furan-2-ylmethyl)-amine (6)

Procedure A, yield 32%. White solid, mp 72–73 °C. ^{1}H NMR (400 MHz, $CDCl_3$): δ 1.52–1.65 (m, 2H, 1H, D_2O exchangeable), 1.83–1.97 (m, 3H), 2.54–2.71 (m, 2H), 3.70–3.87 (m, 2H), 4.01 (s, 3H), 4.04–4.10 (m, 1H), 5.15 (d, J = 4.0 Hz, 1H), 7.17–7.23 (m, 1H), 7.25–7.30 (m, 2H), 7.37–7.44 (m, 2H), 7.60 (dd, J = 9.0, 2.0 Hz, 1H), 7.65 (d, J = 9.0 Hz, 1H), 7.87 (dd, J = 6.4, 2.0 Hz, 1H), 8.12 (s, 1H). ^{13}C NMR (100.6 MHz, $CDCl_3$): δ 25.8, 29.2, 52.6, 53.5, 60.7, 67.9, 78.3, 117.0, 126.7, 127.1, 127.7, 127.8, 128.3, 128.4, 129.3, 129.5, 132.0, 133.9, 134.1, 142.2, 144.1, 160.4. $[M+H]^+$ = *m/e* 427, 429.

5.1.6. [(6-Bromo-2-methoxy-quinolin-3-yl)-phenyl-methyl]-thiophen-2-ylmethyl-amine (7)

Procedure A, yield 28%. Oily liquid, ^{1}H NMR (400 MHz, $CDCl_3$): δ 2.1 (s, 1H, D_2O exchangeable), 3.95 (s, 2H), 3.99 (s, 3H), 5.21 (s, 1H), 6.87–6.90 (m, 1H), 6.93–6.98 (m, 1H), 7.21–7.25 (m, 2H), 7.27–7.31 (m, 2H), 7.41–7.46 (m, 2H), 7.62 (dd, J = 8.8, 2.0 Hz, 1H), 7.67 (d, J = 8.8 Hz, 1H), 7.87 (d, J = 2.0 Hz, 1H), 8.16 (s, 1H). ^{13}C NMR

(100.6 MHz, $CDCl_3$): δ 46.5, 53.6, 59.8, 117.1, 124.4, 124.9, 126.6, 126.7, 127.3, 127.8, 128.39, 128.45, 128.6, 129.6, 132.2, 134.4, 141.7, 143.8, 144.2, 160.4. $[M+H]^+$ = *m/e* 439, 441.

5.1.7. 6-Bromo-2-methoxy-3-{phenyl-[4-(3-trifluoromethyl-phenyl)-piperazin-1-yl]-methyl}-quinoline (8)

Procedure A, yield 49%. White solid, mp 182–183 °C. ^1H NMR (400 MHz, $CDCl_3$): δ 2.51–2.59 (m, 2H), 2.61–2.70 (m, 2H), 3.18–3.30 (m, 4H), 4.03 (s, 3H), 4.77 (s, 1H), 7.0–7.1 (m, 3H), 7.17–7.22 (m, 1H), 7.26–7.36 (m, 3H), 7.38–7.46 (m, 2H), 7.61 (dd, *J* = 9.0, 2 Hz, 1H), 7.65 (d, *J* = 9.0 Hz, 1H), 7.91 (d, *J* = 2 Hz, 1H), 8.27 (s, 1H). ^{13}C NMR (100.6 MHz, $CDCl_3$): δ 48.7, 51.7, 53.7, 67.4, 111.81, 111.85, 115.67, 115.75, 117.2, 118.5, 126.7, 127.4, 128.2, 128.46, 128.54, 128.6, 129.5, 129.6, 132.2, 134.2, 140.4, 144.1, 151.3, 160.6. $[M+H]^+$ = *m/e* 556, 558.

5.1.8. 6-Bromo-2-methoxy-3-(phenyl-piperidin-1-yl-methyl)-quinoline (9)

Procedure A, yield 57%. Light-yellow solid, mp 150–152 °C. ^1H NMR (400 MHz, $CDCl_3$): δ 1.40–1.48 (m, 2H), 1.56–1.70 (m, 4H), 2.25–2.45 (m, 4H), 3.99 (s, 3H), 4.67 (s, 1H), 7.10–7.16 (m, 1H), 7.20–7.25 (m, 2H), 7.31–7.40 (m, 2H), 7.59 (dd, *J* = 8.8, 2.0 Hz, 1H), 7.63 (d, *J* = 8.8 Hz, 1H), 7.90 (d, *J* = 2.0 Hz, 1H), 8.24 (s, 1H). ^{13}C NMR (100.6 MHz, $CDCl_3$): δ 24.7, 26.2, 53.2, 53.5, 68.1, 116.9, 126.86, 126.89, 128.2, 128.4, 128.6, 129.1, 129.6, 131.9, 134.3, 141.3, 143.9, 160.7. $[M+H]^+$ = *m/e* 412, 414.

5.1.9. 6-Bromo-2-methoxy-3-(morpholin-4-yl-phenyl-methyl)-quinoline (10)

Procedure A, yield 59%. Light-yellow solid, mp 150–152 °C. ^1H NMR (400 MHz, $CDCl_3$): δ 2.34–2.4 (m, 2H), 2.47–2.49 (m, 2H), 3.71–3.85 (m, 4H), 4.01 (s, 3H), 4.70 (s, 1H), 7.17 (t, *J* = 7 Hz, 1H), 7.22–7.28 (m, 2H), 7.40 (d, *J* = 7.2 Hz, 2H), 7.60 (dd, *J* = 8.8, 2.0 Hz, 1H), 7.63 (d, *J* = 8.8 Hz, 1H), 7.91 (d, *J* = 1.6 Hz, 1H), 8.25 (s, 1H). ^{13}C NMR (100.6 MHz, $CDCl_3$): δ 52.6, 53.6, 67.1, 67.9, 117.1, 126.7, 127.3, 127.9, 128.3, 128.5, 128.6, 129.5, 132.1, 134.2, 140.1, 144.0, 160.5. $[M+H]^+$ = *m/e* 414, 416.

5.1.10. 6-Bromo-2-methoxy-3-[(5-methyl-tetrazol-1-yl)-phenyl-methyl]-quinoline (11)

Procedure A, yield 50%. White solid, mp 161–162 °C. ^1H NMR (400 MHz, $CDCl_3$): δ 2.58 (s, 3H), 3.98 (s, 3H), 6.93 (s, 1H), 7.22–7.25 (m, 2H), 7.40–7.45 (m, 3H), 7.56 (s, 1H), 7.70 (s, 2H), 7.78 (s, 1H). ^{13}C NMR (100.6 MHz, $CDCl_3$): δ 9.1, 54.2, 59.4, 117.9, 122.6, 125.9, 127.7, 128.7, 129.2, 129.4, 130.0, 133.6, 134.8, 138.2, 145.0, 152.0, 159.1. $[M+H]^+$ = *m/e* 411, 413.

5.1.11. 1-[(6-Bromo-2-methoxy-quinolin-3-yl)-phenyl-methyl]-pyrrolidine-2-carboxylic acid ethyl ester (12)

Procedure A, yield 11%. Light-yellow semi-solid. ^1H NMR (400 MHz, $CDCl_3$): δ 1.05 (t, *J* = 7.2 Hz, 3H), 1.78–2.0 (m, 3H), 2.10–2.16 (m, 1H), 2.45–2.54 (m, 1H), 3.05–3.15 (m, 1H), 3.46–3.54 (m, 1H), 3.74–3.92 (m, 2H), 4.00 (s, 3H), 5.12 (s, 1H), 7.15–7.25 (m, 3H), 7.40 (d, *J* = 6.8 Hz, 2H), 7.60 (dd, *J* = 8.8, 2.0 Hz, 1H), 7.62 (d, *J* = 8.8 Hz, 1H), 7.94 (d, *J* = 2.0 Hz, 1H), 8.36 (s, 1H). ^{13}C NMR (100.6 MHz, $CDCl_3$): δ 14.0, 23.7, 30.3, 52.8, 53.5, 60.1, 63.5, 65.2, 117.0, 126.8, 127.3, 128.0, 128.4, 128.6, 129.0, 129.6, 132.0, 134.8, 141.0, 144.0, 160.1, 174.8. $[M+H]^+$ = *m/e* 470, 472.

5.1.12. 1-[(6-Bromo-2-methoxy-quinolin-3-yl)-phenyl-methyl]-piperidine-4-carboxylic acid ethyl ester (13)

Procedure A, yield 15%. Light-yellow semi-solid, ^1H NMR (400 MHz, $CDCl_3$): δ 1.24 (t, *J* = 7.2 Hz, 3H), 1.76–1.90 (m, 4H), 1.92–2.00 (m, 2H), 2.26–2.33 (m, 1H), 2.70–2.82 (m, 1H), 2.90–3.0 (m, 1H), 3.99 (s, 3H), 4.12 (q, *J* = 7.2 Hz, 2H), 4.70 (s, 1H), 7.12–7.18 (m, 1H), 7.20–7.25 (m, 2H), 7.35–7.40 (m, 2H), 7.59 (dd, *J* = 8.8, 2.0 Hz, 1H), 7.63 (d, *J* = 8.8 Hz, 1H), 7.89 (d, *J* = 2.0 Hz, 1H), 8.22 (s, 1H). ^{13}C NMR (100.6 MHz, $CDCl_3$): δ 13.6, 27.87, 27.93, 40.7, 50.8, 51.1, 53.0, 59.6, 67.0, 116.3, 126.2, 126.5, 127.7, 127.9, 128.2, 128.9, 131.4, 133.5, 140.3, 143.3, 159.9, 174.5. $[M+H]^+$ = *m/e* 484, 486.

5.1.13. [(6-Bromo-2-methoxy-quinolin-3-yl)-phenyl-methyl]-pyridin-4-ylmethyl-amine (14)

Procedure A, yield 17%. Reddish-yellow semi-solid. ^1H NMR (400 MHz, $CDCl_3$): δ 3.78 (s, 2H), 3.99 (s, 3H), 5.15 (s, 1H), 7.25–7.37 (m, 5H), 7.40–7.43 (m, 2H), 7.63 (dd, *J* = 9.0, 2.0 Hz, 1H), 7.66 (d, *J* = 9.0 Hz, 1H), 7.87 (d, *J* = 2.0 Hz, 1H), 8.06 (s, 1H), 8.51–8.60 (m, 2H). ^{13}C NMR (100.6 MHz, $CDCl_3$): δ 50.7, 53.6, 60.2, 117.2, 122.9, 126.5, 127.5, 127.7, 128.48, 128.51, 129.5, 132.3, 134.4, 141.4, 144.2, 149.2, 149.8, 160.3. $[M+H]^+$ = *m/e* 435, 437.

5.1.14. 6-Bromo-3-(indol-1-yl-phenyl-methyl)-2-methoxy-quinoline (15)

Procedure A, yield 10%. White solid, mp 232–233 °C. ^1H NMR (400 MHz, acetone-d_6): δ 3.99 (d, *J* = 9 Hz, 3H), 6.05 (s, 1H), 6.72 (d, *J* = 1.2 Hz, 1H), 6.87–6.91 (m, 1H), 7.07–7.15 (m, 1H), 7.16–7.35 (m, 7H), 7.42 (d, *J* = 8.0 Hz, 1H), 7.64–7.78 (m, 3H), 7.89 (d, *J* = 2.0 Hz, 1H). ^{13}C NMR (100.6 MHz, acetone-d_6): δ 33.9, 45.1, 103.4, 108.4, 109.0, 110.7, 110.8, 113.5, 116.5, 118.2, 118.6, 118.7, 120.1, 120.5, 120.7, 121.4, 121.9, 123.7, 128.1, 129.2, 134.5, 152.8. $[M+H]^+$ = *m/e* 444, 446.

5.1.15. 6-Bromo-3-[(4-nitro-imidazol-)-1-yl-phenyl-methyl]-2-methoxy-quinoline (16)

Procedure A, yield 46%. White solid, mp 79–80 °C. ^1H NMR (400 MHz, $CDCl_3$): δ 4.01 (s, 3H), 6.87 (s, 1H), 7.10–7.14 (m, 2H), 7.37 (s, 1H), 7.40 (d, *J* = 1.4 Hz, 1H), 7.43–7.5 (m, 3H), 7.62 (d, *J* = 1.4 Hz, 1H), 7.74 (s, 2H), 7.8 (s, 1H). ^{13}C NMR (100.6 MHz, $CDCl_3$): δ 54.2, 60.7, 118.1, 119.2, 122.9, 125.5, 127.5, 128.7, 129.4, 129.5, 129.8, 133.9, 135.5, 136.1, 136.7. $[M+H]^+$ = *m/e* 439, 441.

5.1.16. (±)-6-Bromo-2-methoxy-3-(phenyl-pyrazol-1-yl-methyl)-quinoline (17), Procedure B

20% aqueous solution of sodium hydroxide (30 mL) was added to a mixture of compound **2** (2 g, 4.91 mmol), pyrazole (0.33 g, 4.91 mmol) and *n*-tetrabutyl ammonium bromide (0.13 g, 0.49 mmol) in dry toluene (20 mL) and heated to reflux for 2 h. The reaction mixture was cooled to room temperature, diluted with ethyl acetate and the organic layer was separated. The organic layer was washed with water, brine, dried over anhydrous sodium sulfate, filtered and concentrated under vacuum. The crude product was purified by column chromatography on silica gel (100–200 mesh) eluting with hexane–ethyl acetate (9:1) to afford **17** (1.0 g, 51%) as a white solid, mp 142–144 °C. ^1H NMR (400 MHz, $CDCl_3$): δ 3.96 (s, 3H), 6.29 (t, *J* = 2.1 Hz, 1H), 7.03 (s, 1H), 7.11–7.19 (m, 2H), 7.26–7.31 (m, 2H), 7.32–7.38 (m, 3H), 7.61 (d, *J* = 1.7 Hz, 1H), 7.65 (dd, *J* = 8.8, 2.0 Hz, 1H), 7.69 (d, *J* = 8.8 Hz, 1H), 7.75 (d, *J* = 2.0 Hz, 1H). ^{13}C NMR (100.6 MHz, $CDCl_3$): δ 53.9, 63.7, 117.4, 125.6, 126.1, 128.2, 128.4, 128.5, 128.8, 129.75, 129.78, 136.1, 137.8, 140.1, 144.8, 159.7. $[M+H]^+$ = *m/e* 394, 396.

5.1.17. (±)-6-{[(6-Bromo-2-methoxy-quinolin-3-yl)-phenyl-methyl]-amino}-chromen-2-one (18), Procedure C

A mixture of **2** (2 g, 4.91 mmol), 6-aminocoumarin hydrochloride (0.97 g, 4.91 mmol), 1,8-diazabicyclo-[5.4.0]undec-7-ene (0.74 g, 4.91 mmol), and *n*-tetrabutylammonium bromide (0.31 g, 0.98 mmol) in dry toluene (20 mL) were heated under reflux for 14 h. The reaction mixture was cooled to room temperature, poured into water, diluted with ethyl acetate and the organic layer was separated. The organic layer was washed with water followed

by brine, dried over anhydrous sodium sulfate, filtered and concentrated under vacuum. The crude product was purified by column chromatography on silica gel (100–200 mesh) eluting with hexane–ethyl acetate (9:1, v/v) to afford **18** (1.0 g, 42%) as a pale-yellow solid, mp 88–89 °C. ^{1}H NMR (400 MHz, $CDCl_3$): δ 4.02 (s, 3H), 4.33 (d, J = 3.6 Hz, 1H), 5.77 (d, J = 3.6 Hz, 1H), 6.32 (d, J = 9.5 Hz, 1H), 6.44 (d, J = 2.8 Hz, 1H), 6.80 (dd, J = 9.0, 2.8 Hz, 1H), 7.13 (d, J = 9.0 Hz, 1H), 7.29–7.38 (m, 5H), 7.48 (d, J = 5.6 Hz, 1H), 7.65 (dd, J = 9.0, 2.0 Hz, 1H), 7.70 (d, J = 9.0 Hz, 1H), 7.82 (d, J = 2 Hz, 1H), 7.98 (s, 1H). ^{13}C NMR (100.6 MHz, $CDCl_3$): δ 53.8, 57.8, 109.3, 116.8, 117.5, 117.6, 118.7, 119.3, 126.5, 126.6, 127.6, 128.0, 128.5, 128.9, 132.7, 134.5, 140.6, 143.4, 143.6, 144.6, 147.1. $[M+H]^+$ = m/e 486, 488.

5.1.18. (±)-3-(6-Bromo-2-methoxy-quinolin-3-yl)-2-naphtha len-1-yl-3-phenyl-propionic acid ethyl ester (19 and 20), Proce dure D

Sodium hydride (0.031 g, 0.737 mmol) was added to an ice-cold solution of ethyl ester of naphthyl acetic acid (0.115 g, 0.54 mmol) in tetrahydrofuran (4 mL) at 0 °C and stirred at room temperature for 0.5 h. To this reaction mixture was added the solution of **2** (0.20 g, 0.49 mmol) in tetrahydrofuran (4 mL) at 0 °C and stirred at room temperature for 6 h. The reaction mixture was poured into ice-water and extracted into ethyl acetate. The organic layer was washed with brine, dried over anhydrous sodium sulfate, filtered and concentrated under vacuum. The crude product was purified by column chromatography on silica gel (100–200 mesh) eluting with hexane–ethyl acetate (9:1, v/v) to afford **19** (0.05 g, 19%) as a light yellow solid, mp 141–142 °C.

Compound **19**, Upper spot: (10%). ^{1}H NMR (400 MHz, $CDCl_3$): δ 0.91 (t, J = 7.0 Hz, 3H), 3.80–3.94 (m, 2H), 3.95 (s, 3H), 5.50 (d, J = 12.3 Hz, 1H), 5.57 (d, J = 12.3 Hz, 1H), 7.20–7.26 (m, 1H), 7.28–7.34 (m, 3H), 7.44–7.50 (m, 4H), 7.52–7.55 (m, 2H), 7.58–7.64 (m, 3H), 7.70 (d, J = 7.2 Hz, 1H), 7.77 (d, J = 8.1 Hz, 1H), 8.49 (d, J = 8.6 Hz, 1H). ^{13}C NMR (100.6 MHz, $CDCl_3$): δ 13.8, 47.4, 49.8, 53.6, 60.9, 116.9, 122.9, 125.46, 125.53, 125.7, 126.1, 126.4, 127.0, 127.4, 128.0, 128.2, 128.4, 128.7, 129.02, 129.08, 131.9, 132.0, 132.5, 133.8, 134.3, 140.8, 143.7, 160.4, 172.5.

Compound **20**, Lower spot: (9%). ^{1}H NMR (400 MHz, $CDCl_3$): δ 0.92 (t, J = 7.0 Hz, 3H), 3.87–3.98 (m, 2H), 4.06 (s, 3H), 5.37 (d, J = 12.3 Hz, 1H), 5.55 (d, J = 12.2 Hz, 1H), 6.80–6.90 (m, 3H), 7.02–7.06 (m, 2H), 7.38–7.50 (m, 3H), 7.63–7.70 (m, 3H), 7.75 (d, J = 8.0 Hz, 1H), 7.82–7.84 (m, 1H), 7.97 (d, J = 1.8 Hz, 1H), 8.20–8.25 (m, 2H). ^{13}C NMR (100.6 MHz, $CDCl_3$): δ 13.9, 47.8, 53.9, 60.9, 117.2, 123.0, 125.29, 125.33, 126.1, 126.3, 126.5, 127.7, 128.0, 128.4, 128.6, 128.7, 129.1, 129.3, 132.0, 132.2, 132.7, 133.4, 133.7, 139.4, 144.1, 160.6, 172.6.

5.1.19. (±)-2-[(6-Bromo-2-methoxyquinolin-3-yl)-phenyl-methyl]-malonic acid dimethyl ester (21)

Sodium hydride (0.014 g, 0.58 mmol) was added in portions to a stirred solution of dimethyl malonate (0.08 g, 0.67 mmol) in anhydrous tetrahydrofuran (2 mL) at 0 °C and allowed to warm up to room temperature during 0.5 h. The solution of **2** (0.20 g, 0.49 mmol) in tetrahydrofuran (2 mL) was added to the reaction mixture and stirred at room temperature for 4 h. The volatiles were removed under vacuum, poured into ice-water mixture, extracted with dichloromethane, the organic layer was washed with water, brine, dried over anhydrous sodium sulfate, filtered and concentrated under vacuum. The crude product was triturated with *n*-pentane and dried to give the product **21** (0.20 g, 94% yield) as a sticky mass. ^{1}H NMR (400 MHz, $CDCl_3$): δ 3.54 (s, 3H), 3.56 (s, 3H), 4.02 (s, 3H), 4.53 (d, J = 12.0 Hz, 1H), 5.12 (d, J = 12.0 Hz, 1H), 7.13–7.19 (m, 1H), 7.20–7.25 (m, 2H), 7.28–7.32 (m, 2H), 7.59–7.65 (m, 2H), 7.83–7.86 (m, 2H). ^{13}C NMR (100.6 MHz, $CDCl_3$): δ 43.6, 52.3, 52.4, 53.6, 55.0, 116.4, 126.3, 126.9, 127.4, 128.15, 128.18, 128.31, 129.3, 132.0, 134.0, 139.0, 143.2, 159.7, 167.46, 167.50. $[M+H]^+$ = m/e 458, 460.

5.1.20. 2-[(6-Bromo-2-methoxyquinolin-3-yl)-phenyl-methyl]-malonic acid monomethyl ester (22)

Compound **21** (3.0 g, 6.55 mmol) was added to a stirred solution of potassium hydroxide (0.36 g, 6.55 mmol) in water–methanol (1:4, 25 mL) and heated to reflux for 12 h. The volatiles were removed under reduced pressure, poured into ice-water and extracted with diethyl ether. The aqueous layer was separated, acidified with 15% hydrochloric acid solution and extracted with chloroform. The organic layer was washed with brine, dried over anhydrous sodium sulfate, and concentrated under vacuum to obtain the pure **22** (1.40 g, 48%) as a sticky solid. ^{1}H NMR (400 MHz, DMSO-d_6): δ 3.53 (s, 3H), 3.55 (s, 2H), 3.97 (s, 3H), 4.00 (s, 2H), 4.50–4.57 (m, 2H), 5.05–5.08 (d, 2H), 7.12–7.20 (m, 5H), 7.25–7.31 (m, 3H), 7.60–7.62 (m, 3H), 7.81–7.84 (m, 3H), 13.00 (br s, 2H, D_2O exchangeable), (Diastereomeric mixture in 3:2 ratio by ^{1}H NMR spectroscopy). ^{13}C NMR (100.6 MHz, DMSO-d_6): δ 43.5, 43.6, 52.2, 52.3, 53.7, 55.5, 55.6, 116.5, 126.4, 126.8, 126.9, 127.7, 128.0, 128.1, 128.2, 128.26, 128.3, 128.4, 129.2, 129.3, 132.1, 133.9, 134.0, 139.5, 139.7, 143.1, 159.8, 159.9, 168.1, 168.3. $[M+H]^+$ = m/e 444, 446.

5.1.21. Representative Procedure E, for 23, 24, 25, 26, 27 and 28: Preparation of methyl 3-(6-bromo-2-methoxyquinolin-3-yl)-2-(morpholine-4-carbonyl)-3-phenylpropanoate (23 and 24)

3-Morpholin-4-yl-3-oxo-propionic acid methyl ester[20] (0.225 g, 1.22 mmol) was dissolved in dry THF (3 mL) and sodium hydride (0.035 g, 1.47 mmol) was added fractionwise and stirred at 28 °C for 1.5 h. And then compound **2** (0.500 g, 1.22 mmol) was dissolved in dry THF (2 mL) and added to the reaction mixture. Reaction was stirred at 28 °C for 16 h. and monitored by tlc. Reaction was quenched by adding water and THF was removed on rotatory evaporator, extracted with chloroform (2 × 20 mL). Organic layer was washed with water, brine and dried over sodium sulfate and concentrated to get the crude product. This was purified by column chromatography on silica gel (230–400 mesh) eluent: 30% ethyl acetate in hexane to afford the **23** and **24**.

Compound **23**, Upper spot: (0.054 g, 27% yield). White solid, mp 206-208 °C. ^{1}H NMR (400 MHz, $CDCl_3$): δ 3.31–3.35 (m, 1H), 3.37–3.44 (m, 1H), 3.49–3.58 (m, 5H), 3.60–3.63 (m, 2H), 3.67–3.72 (m, 1H), 3.78–3.83 (m, 1H), 4.00 (s, 3H), 4.88 (d, J = 11.8 Hz, 1H), 5.23 (d, J = 11.8 Hz, 1H), 7.13–7.18 (m, 1H), 7.20–7.25 (m, 2H), 7.30–7.34 (m, 2H), 7.60–7.66 (m, 2H), 7.78 (s, 1H), 7.81 (s, 1H). ^{13}C NMR (100.6 MHz, $CDCl_3$): δ 42.8, 46.5, 46.6, 52.1, 52.6, 53.7, 66.6, 66.8, 117.3, 126.4, 127.0, 127.4, 128.34, 128.37, 128.5, 129.1, 132.3, 134.4, 139.4, 144.1, 160.2, 164.9, 168.4. $[M+H]^+$ = m/e 513, 515.

Compound **24**, Lower spot: (0.047 g, 25%). Off-white solid, mp 188–190 °C. ^{1}H NMR (400 MHz, $CDCl_3$): δ 2.95–3.05 (m, 1H), 3.23–3.32 (m, 2H), 3.34–3.44 (m, 1H), 3.48–3.62 (m, 7H), 3.99 (s, 3H), 4.72 (d, J = 12.0 Hz, 1H), 5.24 (d, J = 12.0 Hz, 1H), 7.15–7.25 (m, 5H), 7.60–7.67 (m, 2H), 7.80–7.87 (m, 2H). ^{13}C NMR (100.6 MHz, $CDCl_3$): δ 42.6, 45.5, 46.6, 51.6, 52.7, 53.7, 66.2, 66.5, 117.2, 126.2, 127.2, 127.6, 128.44, 128.48, 128.53, 129.2, 132.3, 133.5, 139.5, 144.1, 160.4, 165.4, 168.4. $[M+H]^+$ = m/e 513, 515.

5.1.22. 3-(6-Bromo-2-methoxy-quinolin-3-yl)-3-phenyl-2-(pyrrolidine-1-carbonyl)-propionic acid methyl ester (25 and 26)

Procedure E. **25**, Upper spot: Yield 14%. Off-white solid, mp 196–198 °C, ^{1}H NMR (400 MHz, $CDCl_3$): δ 1.43–1.49 (m, 2H), 1.67–1.83 (m, 2H), 3.14–3.21 (m, 1H), 3.34–3.40 (m, 1H), 3.54 (s, 3H), 3.58–3.64 (m, 1H), 3.76–3.82 (m, 1H), 4.00 (s, 3H), 4.73 (d, J = 12.0 Hz, 1H), 5.22 (d, J = 12.0 Hz, 1H), 7.11–7.16 (m, 1H), 7.18–

7.24 (m, 2H), 7.34 (d, J = 7.6 Hz, 2H), 7.57–7.65 (m, 2H), 7.79 (d, J = 8.0 Hz, 2H). ^{13}C NMR (100.6 MHz, $CDCl_3$): δ 23.7, 25.5, 44.1, 45.8, 46.3, 52.1, 53.6, 54.4, 116.4, 126.4, 126.7, 128.1, 128.4, 128.5, 129.2, 131.9, 133.4, 139.7, 143.1, 160.0, 163.3, 168.2. $[M+H]^+$ = m/e 497, 499.

Compound **26**, Lower spot: Yield 15%. Off-white solid, mp 196–198 °C. ^{1}H NMR (400 MHz, $CDCl_3$): δ 1.51–1.57 (m, 2H), 1.66–1.82 (m, 2H), 2.95–3.06 (m, 1H), 3.12–3.20 (m, 1H), 3.31–3.4 (m, 1H), 3.53 (s, 3H), 3.58–3.68 (m, 1H), 3.97 (s, 3H), 4.52 (d, J = 12.0 Hz, 1H), 5.23 (d, J = 12.0 Hz, 1H), 7.10–7.20 (m, 3H), 7.20–7.23 (m, 1H), 7.26–7.29 (m, 1H), 7.61–7.68 (m, 2H), 7.8–7.9 (m, 2H). ^{13}C NMR (100.6 MHz, $CDCl_3$): δ 23.6, 25.2, 43.7, 45.4, 46.6, 52.1, 53.5, 53.7, 116.4, 126.4, 126.8, 128.0, 128.2, 128.3, 128.4, 129.3, 131.9, 133.9, 139.2, 143.1, 160.0, 164.4, 168.5. $[M+H]^+$ = m/e 497, 499.

5.1.23. 3-(6-Bromo-2-methoxy-quinolin-3-yl)-3-phenyl-2-(piperidine-1-carbonyl)-propionic acid methyl ester (27 and 28)

Procedure E. **27**, Upper spot: Yield 14%. Off-white solid, mp 218–220 °C. ^{1}H NMR (400 MHz, DMSO-d_6): δ 1.21–1.29 (m, 2H), 1.50–1.60 (m, 4H), 3.38–3.43 (m, 2H), 3.43 (s, 1H), 3.96 (s, 3H), 5.10 (s, 2H), 7.13–7.19 (m, 1H), 7.21–7.28 (m, 2H), 7.39–7.45 (m, 2H), 7.60–7.65 (m, 1H), 7.68–7.74 (m, 1H), 7.97 (s, 1H), 8.37 (s, 1H). ^{13}C NMR (100.6 MHz, DMSO-d_6): δ 23.8, 25.4, 26.2, 42.8, 44.3, 46.4, 51.9, 52.1, 53.7, 116.5, 126.4, 126.8, 128.1, 128.5, 128.7, 129.0, 132.0, 133.3, 139.7, 143.1, 160.1, 163.5, 168.5. $[M+H]^+$ = m/e 511, 513.

Compound **28**, Lower spot: Yield 13%. Off-white solid, mp 209–211 °C. ^{1}H NMR (400 MHz, DMSO-d_6): δ 1.18–1.24 (m, 1H), 1.28–1.33 (m, 2H), 1.36–1.47 (m, 3H), 1.51–1.70 (m, 1H), 3.05–3.11 (m, 1H), 3.29–3.43 (m, 2H), 3.45 (s, 3H), 3.96 (s, 3H), 5.05–5.17 (m, 2H), 7.13–7.17 (m, 1H), 7.22 (t, J = 8.0 Hz, 2H), 7.26–7.31 (m, 2H), 7.65 (d, J = 9.0 Hz, 1H), 7.72 (dd, J = 9.0, 2.0 Hz, 1H), 8.02 (d, J = 2.0 Hz, 1H), 8.60 (s, 1H). ^{13}C NMR (100.6 MHz, DMSO-d_6): δ 24.3, 25.4, 26.1, 43.6, 45.4, 47.3, 51.9, 52.6, 53.7, 117.1, 126.3, 126.9, 128.0, 128.3, 128.5, 129.2, 132.2, 133.6, 139.8, 144.1, 160.5, 164.7, 168.8. $[M+H]^+$ = m/e 511, 513.

5.1.24. Representative Procedure F, for 29, 30 and 31: Preparation of 3-(6-bromo-2-methoxy-quinolin-3-yl)-3-phenyl-2-(pyrazole-1-carbonyl)-propionic acid methyl ester (29)

To a stirred solution of compound **22** (0.600 g, 1.35 mmol), in dry tetrahydrofuran (10 mL) was added *N*-hydroxybenzotriazole (0.100 g, 1.48 mmol), pyrazole (0.100 g, 1.48 mmol), EDC·HCl (0.309 g, 1.62 mmol) and diisopropyl amine (0.22 mL, 1.62 mmol) at 0 °C and stirred at room temperature for 16 h. The volatiles were removed under reduced pressure, poured into ice-water and extracted with chloroform. The organic layer was washed with brine, dried over anhydrous sodium sulfate and concentrated under vacuum. The crude product was purified by column chromatography on silica gel (230–400 mesh) eluent: hexane–ethyl acetate (7:3) to get pure product **29** as a diastereomeric mixture. Yield 14%. Off-white solid, mp 180–182 °C. ^{1}H NMR (400 MHz, $CDCl_3$): δ 3.46 (s, 3H), 3.50 (s, 3H), 3.98 (s, 3H), 4.05 (s, 3H), 5.35 (d, J = 3.6 Hz, 1H), 5.38 (d, J = 4.0 Hz, 1H), 5.95 (d, J = 12.0 Hz, 1H), 6.05 (d, J = 12.0 Hz, 1H), 6.37–6.41 (m, 1H), 6.42–6.46 (m, 1H), 7.04–7.10 (m, 1H), 7.11–7.16 (m. 2H), 7.16–7.21 (m, 1H), 7.23–7.28 (m, 1H), 7.29–7.32 (m, 3H), 7.36–7.40 (m, 2H), 7.60–7.65 (m, 2H), 7.65–7.68 (m, 1H), 7.76 (s, 1H), 7.83 (s, 1H), 7.86 (s, 2H), 7.96 (s, 1H), 8.07 (dd, J = 10.4, 3.2 Hz, 2H). ^{13}C NMR (100.6 MHz, $CDCl_3$): δ 29.7, 45.1, 52.8, 52.9, 53.0, 110.5, 117.1, 126.2, 127.0, 127.1, 128.3, 128.4, 128.5, 128.7, 129.2, 132.3, 133.5, 134.4, 138.8, 144.1, 144.6, 160.2, 165.8, 167.6. $[M+H]^+$ = m/e 494, 496.

5.1.25. 3-(6-Bromo-2-methoxy-quinolin-3-yl)-3-phenyl-2-[4-(3-trifluoromethyl-phenyl)-piperazine-1-carbonyl]-propionic acid methyl ester (30 and 31)

Procedure F. **30**, Upper spot: Yield 30%. Off-white solid, mp 195–196 °C. ^{1}H NMR (400 MHz, $CDCl_3$): δ 2.94–3.02 (m, 2H), 3.08–3.22 (m, 2H), 3.44–3.52 (m, 1H), 3.55 (s, 3H), 3.73–3.84 (m, 2H), 3.85–3.99 (m, 1H), 4.02 (s, 3H), 4.79 (d, J = 12.0 Hz, 1H), 5.27 (d, J = 12.0 Hz, 1H), 6.93–7.06 (m, 2H), 7.11 (d, J = 8.0 Hz, 2H), 7.19 (t, J = 4.0 Hz, 2H), 7.25–7.30 (m, 2H), 7.34 (m, 1H), 7.60–7.66 (m, 2H), 7.91–7.98 (m, 2H). ^{13}C NMR (100.6 MHz, $CDCl_3$): δ 42.1, 45.7, 46.6, 48.9, 49.3, 52.4, 52.7, 53.7, 112.78, 112.82, 112.87, 112.91, 116.86, 116.90, 116.94, 117.0, 117.3, 119.4, 125.5, 126.4, 127.1, 127.5, 128.37, 128.39, 128.5, 129.1, 139.4, 144.1, 150.8, 160.2, 164.8, 168.4. $[M+H]^+$ = m/e 656, 658.

31, Lower Spot: Yield 28%. Off-white solid, mp 194–196 °C. ^{1}H NMR (400 MHz, $CDCl_3$): δ 2.53–2.57 (m, 1H), 2.68–2.79 (m, 1H), 3.01–3.23 (m, 3H), 3.48–3.62 (m, 4H), 3.67–3.81 (m, 2H), 4.00 (s, 3H), 4.79 (d, J = 12.0 Hz, 1H), 5.27 (d, J = 12.0 Hz, 1H), 6.95–6.99 (m, 2H), 7.11 (d, J = 7.2 Hz, 2H), 7.20 (t, J = 7.2 Hz, 2H), 7.21–7.28 (m, 2H), 7.34 (t, J = 8.0 Hz, 1H), 7.62–7.66 (m, 2H), 7.85–7.88 (m, 2H). ^{13}C NMR (100.6 MHz, $CDCl_3$): δ 41.4, 43.7, 45.2, 47.5, 47.7, 50.1, 52.3, 53.8, 54.9, 111.39, 111.43, 111.5, 115.2, 115.24, 116.5, 119.1, 126.4, 126.7, 128.2, 128.5, 128.6, 129.8, 130.0, 132.0, 133.8, 139.5, 143.1, 150.7, 160.1, 165.1, 168.5. $[M+H]^+$ = m/e 656, 658.

5.2. Biological analysis

5.2.1. Cytotoxicity assay

Cellular viability in the presence and absence of test compounds was determined by MTT (3-(4,5-dimethylthiazol-2yl)-2,5-dimethyl tetrazolium bromide; Sigma–Aldrich) microcultured tetrazolium assay.[21,22] The cells (monocytic cell line, THP-1) were plated in flat-bottomed 96-well plates (10,000 cells/100 μL) and cultured in controlled atmosphere (5% CO_2 at 37 °C). Cells were cultured in the presence of medium along with DMSO (live controls). Different concentrations of compounds (1 μg/100 μL and 10 μg/100 μL) were added to the cells. After 24 h and 72 h, stock MTT solution (5 mg/mL) was added to the culture. Cells were again kept in CO_2 incubator for 4 h. After 4 h, 100 μL isopropanol was added and mixed 5–6 times. The absorbance was read at 540 nm in a plate reader (Bio-Rad—450). The results were represented as percentage cell viability (Table 4). All the experiments were carried out in triplicates and the readings were the mean of three readings.

5.3. Computational methods

5.3.1. Homology modelling

Subunit a (gi:54040843) sequence of the *M. tuberculosis* ATP synthase was queried in BLAST[23] search at NCBI (http://www.ncbi.nlm.nih.gov/). All parameters were used with their default values during the BLAST search. The obtained sequences were aligned using CLUSTALx[24] multiple sequence alignment methodology (aln1). At the same time, corresponding subunit a sequence of the *E. coli* ATP synthase was also subjected to BLAST search. Obtained sequences were aligned using secondary structure definition in CLUSTALx for the transmembrane helix regions as known from solved-structure of ATP synthase a/c subunits from *E. coli* (PDB Id: 1C17)(aln2). The pre-aligned *M. tuberculosis* sequences (aln1) were then added to the structure-sequence alignment of *E. coli* sequences (aln2) using profile-to-profile methodology in CLUSTALx to yield alignment (aln3). Same process was repeated for the subunit c of *M. tuberculosis*. From the larger alignment, the sequences of subunit a and c of *M. tuberculosis* and *E. coli* were extracted. This extracted alignment was used for generating homology models of combined subunit a–c complex, where

E. coli a–c subunit sequences were used as template sequences for generating the homology model of *M. tuberculosis* target sequences. Finally, the homology model consisted of 2 c-subunits and 1 a-subunit having inter-subunit contacts. MODELLER[25] was used for generating the homology models. On visual inspection, models were found to be reasonable and root mean square deviation for Cα atoms in transmembrane helix regions was found to be 1.20 Å (for a subunit) and 0.84 Å (for c subunit) between template structure and homology model. The model with lowest value of MODELLER OBJECTIVE FUNCTION was selected and was energy minimised (Conjugate Gradients Minimisation for 2000 steps in NAMD[26]) to remove the steric clashes. The critical residues of the subunit a and c were kept in pre-defined protonation states during the whole process. Glu-61 (subunit c) protonated: Glu-61 (subunit c) deprotonated: Arg 186 (subunit a): protonated. Satisfaction of such charges in the membrane domain is absolutely necessary, owing to high free-energy cost of putting a charge in membrane dielectric. We also assume here that proton translocation mechanism of the ATP synthase of both *E. coli* and *M. tuberculosis* is same.

5.3.2. Molecular modelling

DARQ molecule and its four configurations were sketched in ChemOffice[27] and were subjected to energy minimisation. Flexible terminal amine of *RS* stereoisomer was subjected to conformational analysis to obtain an intramolecular H-bond. Other compounds were sketched and were subjected to conformational analysis and subsequent energy minimisation in Ghemical.[28] The Gasteiger–Marsili[29] partial atomic charge model was used for DARQ. The charges were made into CHARMM[30] topology files using Paratool.[31] Various parameters were constructed ad hoc for bond lengths, angles and dihedrals of the DARQ to be used in further analysis. As we are to compare the energetics of different stereoisomers of same compound (DARQ), we assume the inconsistencies in calculations cancel out.

5.3.3. Docking

Docking simulations were performed using AUTODOCK (version 4).[32] The ligands were docked into a grid (of $64 \times 42 \times 44$ Å^3) with spacing 0.375 Å centred at a position located in the vicinity of crucial residues R186 (subunit a) and E61 (subunit c), which has also been suggested to be the binding site of DARQ.[11] Lamarckian genetic algorithm docking methodology available in AutoDock was used for docking simulations. In total 100 runs were made, with a population size of 250 and 25 million energy evaluations. Initial coordinates (*tran0* option in AutoDock) were set to the defined grid centre. These parameters were set using the AutoDock Tools (ADT).[33] The values of parameters were used after an initial testing with various runs and idea was to obtain convergence in the calculations. However, even after playing with AutoDock parameters, like larger population size and energy evaluations, we were not able to achieve convergence within the limits of our in-house computational power, probably owing to the complexity of the protein and ligand systems. We selected protein–ligand docked complex based on various parameters; AutoDock clustering scenario (root mean square based), AutoDock Intermolecular Energy and most importantly the reasonableness of the interactions between ligand and protein. Because of non-convergent results in some cases, we decided to choose the results based on structural analysis of the docked complexes, rather than AutoDock specific parameters only. Selected protein–ligand complex (only DARQ molecule) were further subjected to 15,000 steps of Conjugagte Gradients energy minimisation in NAMD to refine the system as well as remove steric clashes. The interaction energies were calculated between the ligand and protein (comprising of van der Waals and electrostatic terms) of the minimised complexes.

In large, we did not perform molecular dynamics simulations over the complex or the homology model, for which we assume usually deteriorate the system, specially in the absence of good forcefield parameterisation. The general forcefield parameterisation for this diarylquinoline class of compounds will be used in future to obtain better energetics and structural and interaction analysis.

All structural analysis was performed using VMD.[34] Simulations were run on a workstation having AMD Opteron Processor (2.4 GHz Dual Core) running with Red Hat Enterprise Linux 5.

Acknowledgement

We thank Dr. Anjlina Wali, Institute of Molecular Medicine, for cytotoxicity screening of compounds.

Supplementary data

Supplementary data (characterization data (^{1}H NMR, ^{13}C NMR, DEPT) for all compounds and Tables S1, S2 and S3 are included) associated with this article can be found, in the online version, at doi:10.1016/j.bmc.2009.02.026.

References and notes

1. (a) World Health Organization. In *Anti-tuberculosis Drug Resistance in the World.* The WHO/IUALTD Global project on Anti-Tuberculosis Drug Resistance Surveillance. World Health Organization (Publication # WHO/TB/97.229), Geneva, Switzerland, 1997.; (b) Nakata, K.; Honda, T. N.; Weiden, M.; Keicho, N. *Kekkaku* **2000**, *75*, 547.
2. (a) Snider, D. E.; Raviglione, M.; Kochi, A. In *Global Burden of Tuberculosis, Tuberculosis: Pathogenesis, Protection and Control*; Bloom, B., Ed.; ASM: Washington, DC, 1994; p 3; (b) Dye, C.; Scheele, S.; Dolin, P.; Pathania, V.; Raviglione, M. C. *J. Am. Med. Assoc.* **1999**, *282*, 677.
3. De Cock, K. M.; Chaisson, R. E. *Int. J. Tuberc. Lung Dis.* **1999**, *3*, 457.
4. Corbett, E. L.; Watt, C. J.; Walker, N.; Maher, D.; Williams, B. G.; Raviglione, M. C.; Dye, C. *Arch. Int. Med.* **2003**, *163*, 1009.
5. World Health Organization. Global tuberculosis control: surveillance, planning, financing. WHO report 2004; World Health Organization, Geneva, Switzerland.
6. Mario, C. R.; Smith, I. M. *N. Eng. J. Med.* **2007**, *356*, 656.
7. Andries, K.; Verhasselt, P.; Guillemont, J.; Gohlmann, W. H.; Neefs, J.; Winkler, J.; Timmerman, P.; Zhu, M.; Lee, E.; Williams, P.; Chaffoy, D.; Huitric, E.; Hoffner, S.; Cambau, E.; Pernot, C.; Lounis, N.; Jarlier, V. *Science* **2005**, *307*, 223.
8. Petrella, S.; Cambau, E.; Chauffour, A.; Andries, K.; Jarlier, V.; Sougakoff, W. *Antimicrob. Agents Chemother.* **2006**, *50*, 2853.
9. Rastogi, V.; Girvin, M. *Nature* **1999**, *402*, 263.
10. Gaurrand, S.; Desjardines, S.; Meyer, C.; Bonnet, P.; Argoullon, J.; Oulyadi, H.; Guillemont, J. *Chem. Biol. Drug. Des.* **2006**, *68*, 77.
11. Jonge, M. R.; Koymans, L.; Guillemont, J.; Koul, A.; Andries, K. *Proteins* **2007**, *67*, 971.
12. Jaya Kishore, V.; Labore, S. V.; Shaikh, M. M.; Nageswar Rao, V.; Kulkarni, G. M.; Sarmah, M. P.; Upadhayaya, R. S.; Chattopadhaya, J. Unpublished results.
13. Pathak, R.; Madapa, S.; Batra, S. *Tetrahedron* **2007**, *63*, 451.
14. Bellier, B.; Million, M.-E.; DaNascimento, S.; Meudal, H.; Kellou, S.; Maigret, B.; Garbay, C. *J. Med. Chem.* **2000**, *43*, 3614.
15. Han, S.-Y.; Kim, Y.-A. *Tetrahedron* **2004**, *60*, 2447.
16. Vanitha, J. D.; Paramasivan, C. N. *Mycobacteriology* **2004**, *49*, 179.
17. Reis, R. S.; Neves, I., Jr.; Lourenco, S. L. S.; Fonseca, L. S.; Lourenco, M. C. S. *J. Clin. Microbiol.* **2004**, *42*, 2247.
18. Bloom, B. R.; Murray, C. J. *Science* **1992**, *257*, 1055.
19. Armarego, W. L. F.; Chai, C. L. L. *Purification of Laboratory Chemicals*, 5th ed., Butterworth Heinemann, 2003.
20. Angelastro, M. R.; Baugh, L. E.; Bey, P.; Burkhart, J. P.; Chen, T.-M. *J. Med. Chem.* **1994**, *37*, 4538.
21. Souza, M. C.; Siani, A. C.; Ramos, M. F. S.; Limas, O. M., Jr.; Henriques, M. G. M. O. *Pharmazie* **2003**, *58*, 582.
22. Carvalho, M. V.; Penido, C.; Siani, A. C.; Valente, L. M. M.; Henriques, M. G. M. O. *Gmelin Inflammopharmacol.* **2006**, *14*, 48.
23. Altschul, S. F.; Gish, W.; Miller, W.; Myers, E. W.; Lipman, D. J. *J. Mol. Biol.* **1990**, *215*, 403.
24. Thompson, J. D.; Gibson, T. J.; Plewniak, F.; Jeanmougin, F.; Higgins, D. G. *Nucleic Acids Res.* **1997**, *25*, 4876.
25. Sali, A.; Blundell, T. L. *J. Mol. Biol.* **1993**, *234*, 779.
26. Kalé, L.; Skeel, R.; Bhandarkar, M.; Brunner, R.; Gursoy, A.; Krawetz, N.; Phillips, J.; Shinozaki, A.; Varadarajan, K.; Schulten, K. *J. Comput. Phys.* **1999**, *151*, 283.
27. ChemOffice Version 6. CambridgeSoft, Cambridge, MA, USA.
28. Hassinen, T.; Peräkylä, M. *J. Comp. Chem.* **2001**, *22*, 1229. http://www.uku.fi/~thassine/projects/ghemical/.

29. Gasteiger, J.; Marsili, M. *Tetrahedron Lett.* **1978**, *34*, 3181.
30. Brooks, B. R.; Bruccoleri, R. E.; Olafson, B. D.; States, D. J.; Swaminathan, S.; Karplus, M. *J. Comp. Chem.* **1983**, *4*, 187.
31. Saam, J.; Ivanov, I.; Walther, M.; Holzhutter, H.; Kuhn, H. *Proc. Nat. Acad. Sci. U.S.A.* **2007**, *104*, 13319.
32. Morris, G. M.; Goodsell, D. S.; Halliday, R. S.; Huey, R.; Hart, W. E.; Belew, R. K.; Olson, A. J. *J. Comp. Chem.* **1998**, *19*, 1639.
33. Sanner, M. F. *J. Mol. Graph. Mod.* **1999**, *17*, 57. http://mgltools.scripps.edu.
34. Humphrey, W.; Dalke, A.; Schulten, K. *J. Mol. Graph.* **1996**, *14*, 33.
35. Box, V. G. S.; Marinovic, N.; Yiannikouros, G. P. *Heterocycles* **1991**, *32*, 245.
36. Texier, F.; Marchant, E.; Carrie, R. *Tetrahedron* **1974**, *30*, 3185.